Hindawi Publishing Corporation
Journal of Biomedicine and Biotechnology
Volume 2011, Article ID 252141, 10 pages
doi:10.1155/2011/252141

Methodology Report

Assessment of Elastase-Induced Murine Abdominal Aortic Aneurysms: Comparison of Ultrasound Imaging with *In Situ* Video Microscopy

Junya Azuma,[1] Lars Maegdefessel,[1] Toshiro Kitagawa,[1] Ronald L. Dalman,[2] Michael V. McConnell,[1] and Philip S. Tsao[3]

[1] *Division of Cardiovascular Medicine, Stanford University school of Medicine, CA, USA*
[2] *Department of Vascular Surgery, Stanford University school of Medicine, CA, USA*
[3] *Stanford University school of Medicine, 300 Pasteur Drive, Stanford, CA 94305-5406, USA*

Correspondence should be addressed to Junya Azuma, jazuma@stanford.edu and Philip S. Tsao, ptsao@stanford.edu

Received 15 September 2010; Revised 1 December 2010; Accepted 20 December 2010

Academic Editor: Monica Fedele

Aims. The aim of this study was to definitively assess the validity of noninvasive high-frequency ultrasound (US) measurements of aortic luminal diameter (ALD) in a murine model of elastase-induced abdominal aortic aneurysm in comparison with in situ video microscopy (VM). *Methods*. C57BL/6 mice underwent transient perfusion of the aorta with either elastase ($n = 20$: Elastase group) or saline ($n = 10$: Sham). Unoperated mice ($n = 10$) were also studied. *Results*. ALD measurements by US had excellent linear correlation and absolute agreement with that by VM in both Control (unoperated or sham-operated mice) and elastase groups ($r = 0.96$, intraclass correlation coefficient (ICC) = 0.88 and $r = 0.93$, ICC = 0.92, resp.). Bland-Altman analysis of US compared with VM measurements in both groups indicated good agreement, however US measurements were slightly but significantly higher than VM measurements in the control group (mean bias 0.039 mm, $P < .05$). Linear regression analysis revealed excellent correlation between US and VM measurements in both groups. ($R^2 = 0.91$ in Control group, $R^2 = 0.85$ in elastase group.) The reliability of US measurements was also confirmed by ex vivo histological measurements. *Conclusions.* High-frequency US provides reliable ALD measurements in developing murine abdominal aortic aneurysms.

1. Introduction

Human abdominal aortic aneurysm (AAA) is defined as a pathologic dilatation of the abdominal aortic diameter >30 mm. AAAs are a significant cause of morbidity and mortality in the United States and worldwide. AAAs account for approximately 9,000–30,000 deaths, 150,000 inpatient hospitalizations, and 30,000 open repairs per year in the United States [1].

The mechanism of AAA formation is an active area of basic and clinical investigation. Considerable research on the pathogenesis of AAAs has utilized a variety of mouse models. Three contemporary murine models involve either intraluminal elastase infusion [2], periadventitial application of calcium chloride [3], or chronic angiotensin II infusions in hyperlipidemic animals [4]. Transient intraluminal perfusion of the abdominal aorta with porcine pancreatic elastase has provided the most widely used animal model of AAAs since it was first described in rats by Anidjar et al. [5]. This model was later adapted to mice by Pyo and colleagues [2]. The aortic dilatation in this model is associated with transmural aortic wall infiltration by mononuclear phagocytes, increased local expression of elastolytic matrix metalloproteinases, and pronounced circumferential destruction of the medial elastic lamellae, mimicking much of the human pathology. In addition, recent evidence indicates an additional role of SMC phenotypic modulation in experimental murine and human aneurysms [6].

Since AAA luminal diameter is the most important clinical determinant for risk of rupture, accurate measurement of aneurysm diameter in the mouse model is essential for study interpretation. Despite the extensive efforts made in developing murine AAA models, the methods for quantifying disease progression remain inadequate. Most notably in elastase infusion aneurysm models, either a calibrated ocular grid to measure external AAA diameter or histomorphometry with a "shrinkage index" to estimate luminal diameter has been used [7–9].

A recently developed high-frequency US imaging system by VisualSonics (Toronto, ON, Canada) has increased spatial resolution making it possible and practical to quantify murine vascular dimensions noninvasively [10, 11]. This methodology has been used to monitor AAA development in the angiotensin II infusion model in apoE(−/−) mice (AngII-apoE(−/−) model) [12]. However, this model is now recognized to create focal segmental dissections of the suprarenal aorta that are associated with pseudoaneurysms in addition to the abdominal lumen [13, 14]. As such, there have been few reports in mice to date using ultrasound techniques that distinguish between the true and "false" (pseudoaneurysm) lumen. Thus, the current study was designed to assess the utility of high-frequency US measurements of ALD in comparison to VM in the murine elastase AAA model in which pseudoaneurysms are not commonly seen. The fidelity of US measurements was also confirmed by *in situ* VM measurements as well as *ex vivo* histological assessments. The ALDs in previous reports were measured without the clear definition of pseudoaneurysm and histological assessments were not performed enough. Moreover, *in vivo* VM measurement is inevitable to assess the validity of *in vivo* US measurement.

2. Materials and Methods

2.1. Experimental Animals. All protocols were approved by the Administrative Panel on Laboratory Animal Care at Stanford University and were performed in accordance with the guidelines of the American Association for the Accreditation of Laboratory Animal Care. A total of 40 male C57Bl/6 wild-type mice were obtained from Jackson Laboratories (Bar Harbor, ME, USA). Animals were maintained on a normal chow diet (Purina labdiet HMR3000) containing 26% protein, 14% fat, and 60% carbohydrate by calorie count, given free access to tap water, and housed in a room with a 12 : 12-hour light-dark cycle and a temperature of 22°C.

2.2. Elastase-Induced AAA Model. Mice were anesthetized using 2.0–2.5% isoflurane and a laparotomy was performed under sterile conditions, as previously described in [2, 15]. The abdominal aorta was isolated from the level of the renal vein to the bifurcation with the assistance of an operating stereomicroscope (Leica). After placing temporary ligatures around the proximal and distal aorta, an aortotomy was created at the bifurcation with the tip of a 30-gauge needle. An insertion catheter was created by MicroRenathane Implantation Tubing (MRE010 and MRE025; Braintree Scientific, Inc., Braintree, MA) for infusion into the aorta. The catheter was introduced through the aortotomy, secured, and the aortic lumen was infused for 5 minutes at 100 mmHg with saline ($n = 10$) or saline containing type I porcine pancreatic elastase (1.5 U/mL; Sigma Chemical Co; $n = 20$). After removing the infusion catheter, the aortotomy was repaired without constriction of the lumen. Upon recovery, animals were allowed free access to food and water for 28 days.

2.3. Aortic Diameter Measurements by Ultrasound Imaging. Twenty-eight days after saline or elastase perfusion, ultrasound imaging was performed on the operated mice to assess ALD. Age-matched mice that did not receive saline or elastase perfusion were also studied with ultrasound and videomicroscopic imaging ($n = 10$). Mice were anesthetized using 2.0% isoflurane, and hair was removed from the abdomen by using depilatory cream (Nair; Church & Dwight Co, Inc; Princeton, NJ). Mice were laid supine on a heated table and warmed ultrasound transmission gel was placed on the abdomen. Two-dimensional B mode imaging was performed using a real-time microvisualization scan head (RMV 704) with a central frequency of 40 MHz, frame rate of 30 Hz, a focal length of 6 mm, and a 20×20 mm field of view (Visualsonics; Toronto, Canada). Transverse image scans were performed and cine loops of 300 frames were acquired throughout the infrarenal region of the abdominal aorta. The acquired images were stored digitally on a built-in hard drive for offline analysis for maximal ALD. All aortic diameters were measured in anterioposterior direction during the diastolic phase. US image analysis was performed using the accompanying Vevo 770 software (Figure 1). Measurements were repeated on two separate occasions using random selection of each dataset and operator blinding to prevent recall bias. All measurements were collected by one observer to limit bias while the results were analyzed and collated by a second independent observer who was blinded to the treatment groups.

2.4. Aortic Diameter Measurements by Video Microscope. Immediately after US images were taken, the infrarenal area was exposed by laparotomy and the aorta was carefully dissected of connective tissue to allow visualization of the inner lumen of AAA, avoiding major bleeding or induction of spasm. Images were captured using a high-resolution digital camera (DFC400, Leica) and analyzed with a micrometer to document the ALD. VM image analysis was performed using the Image-Pro Express V6.0 (Media Cybernetics, Inc. Bethesda, MD). The diaphanous nature of the mouse aortic wall permitted visual detection of blood flow and therefore the aortic lumen. Digital zoom was used to verify the inner luminal wall of the aorta (Figure 1(h)). Inner luminal walls were then digitally traced and maximum diameter was measured in the transverse direction (Figures 1(e), 1(f), and 1(g)).

2.5. Aortic Tissue Acquisition and Histology. Histological staining was performed in the same region of abdominal

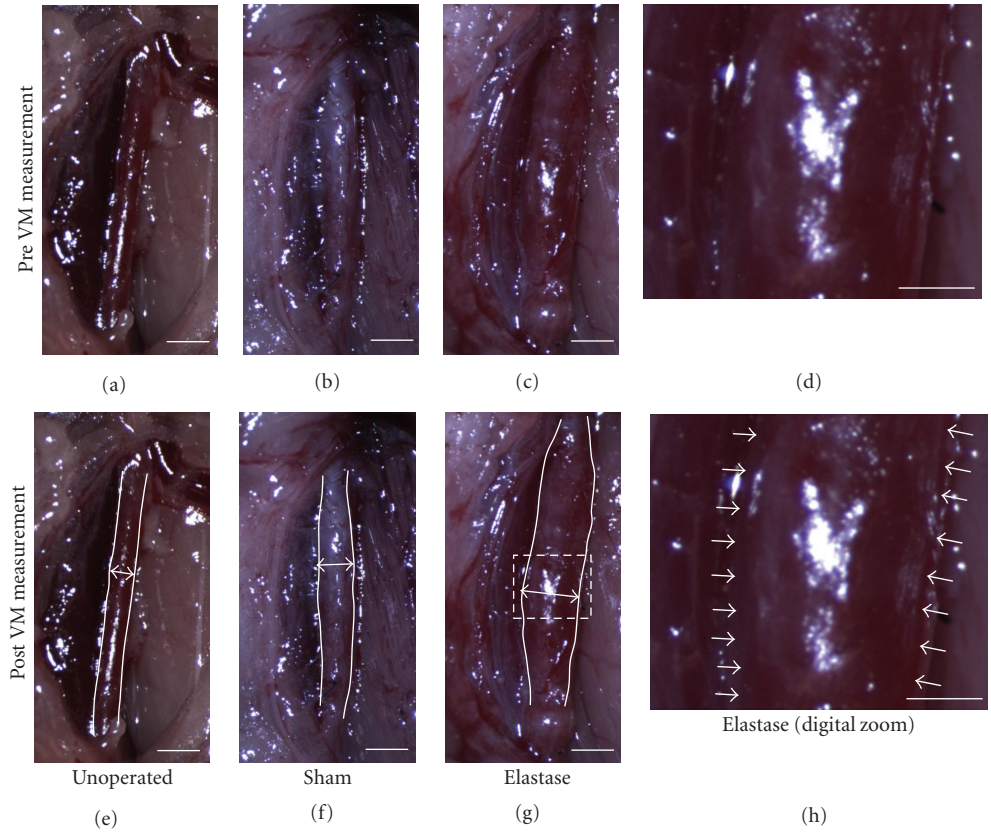

Figure 1: Aortic diameter measurement by VM. Inner lumen of the region of interest was traced and maximum diameter was measured in the transverse direction ((e), (f), (g)). (h) White arrows demarcate the luminal edge of aorta perfused with elastase. Black bars = 1 mm. White bars = 500 μm.

aorta that was imaged in order to obtain morphometric data to correlate with both US and VM measurements. After VM images were taken, the mice were euthanized and perfused at a constant pressure of 100 mmHg through the heart with saline followed by warm (37°C) agarose gel (Agarose SF; Amresco, Solon, OH) diluted in saline (3% w/v). After the agarose had solidified, the abdominal aorta was dissected free from the surrounding connective tissue and fixed in 4% formalin. Isolated tissue was then dehydrated through a graded sucrose series and subsequently embedded in OCT blocks. Aortic tissue was then segmented into 4 (0.5 mm spacing) 7 μm thick serial sections from the left renal artery to the bifurcation and stained with hematoxylin and eosin. Histological image analysis was performed using Image J (National Institute of Mental Health, Bethesda, MD). ALD was estimated by measuring the luminal circumference at each of the 4 sections with the maximal value correlating to the largest location. Maximal ALD was then calculated from circumferential length with the following equation: diameter = circumferential length/pi.

Some sections were assessed for histopathology with Elastic-van Gieson (Sigma, St. Louis, MO) and Masson's trichrome stain (Richard Allan Scientific, Kalamazoo, MI). In addition, smooth muscle alpha-actin content was determined by immunohistochemical analysis. In brief, sections were initially incubated with 5% normal goat serum at room temperature to reduce nonspecific binding before being incubated with the primary antibody against SM alpha-actin (ABCAM, Inc, Cambridge, MA) overnight at 4°C. After washing in phosphate-buffered saline, primary antibodies were detected with the Vectastain ABC Kit (Vector Laboratories, Inc, Burlingame, CA). Visualization was aided by AEC (DAKO North America, Inc, Carpinteria, CA) while counterstaining was performed with Mayer's Hematoxylin (Sigma, St. Louis, MO). Negative controls were run with the omission of the primary antibody.

2.6. Statistical Analysis. Linear association between the ALD acquisition methods was analyzed by Pearson's correlation coefficient. Agreement between US and VM was quantified through Intraclass Correlation Coefficient (ICC) for absolute agreement by taking into consideration the variance between observations and subjects. The ICC is the proportion of the total variance caused by the variation between subjects such that, in this study, an ICC of 1 denotes that the total variance is purely a result of the variation between aortas, whereas an ICC of 0 suggests that the total variance is entirely related to the variation between observations or caused by measurement error. In general, an ICC >0.75 is considered a "good level of agreement" between serial

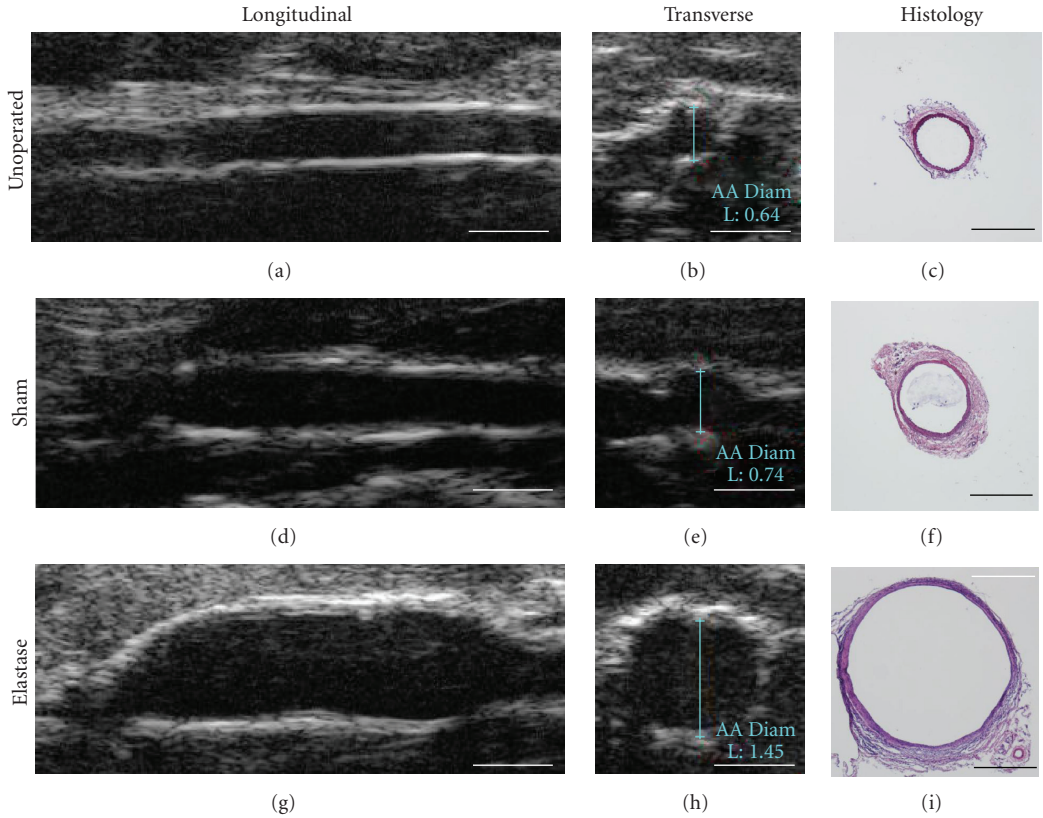

Figure 2: Representative examples of US images of abdominal aorta obtained noninvasively by high-frequency US imaging system (Vevo 770) in the longitudinal ((a), (d), (g)) and transverse ((b), (e), (h)) directions. Double-headed arrows give the anterioposterior direction. Corresponding histological cross-sections of the infrarenal aorta stained with H&E are shown in (c), (f), and (i). Black bars = 500 μm, white bars = 1 mm.

measurements or single measures by different observers [16]. Intraobserver variability was also analyzed with ICC for absolute agreement. The statistical difference between ICCs was evaluated through the application of Fisher's Z transformation, with significance determined with the t statistic.

Since the ICC may have inherent bias due to homogeneity of the sample groups, the "limits of agreement" method described by Bland and Altman (1986), where a scatter plot of the differences between measurements against the mean of the measurements was also used. Paired Student's t-tests were used to compare the measurements between the two different methods, while the correlation between the two methods was determined by linear regression. All data are expressed as means and standard error of the mean. For all analyses, a P value <.05 was considered statistically significant. The statistical analysis was performed with SPSS 16.0 (SPSS, Inc., Chicago, IL, USA).

3. Results

3.1. Aortic Structure Assessed by Histology. Histological assessment was performed to confirm the difference in medial wall structure between the groups. H&E staining in all samples showed no existence of pseudoaneurysms. Elastic van Gieson staining demonstrated wavy and thick elastic sheets in medial layer (Figure 3(a)). Elastin layers were partially stretched but the thickness is preserved well in sham-operated mice (Figure 3(b)). In contrast, elastase perfusion resulted in destruction of the medial elastin layer (Figure 3(c)). Masson's trichrome staining showed intense deposition of extracellular matrix among VSMCs of elastase-perfused animals (Figure 3(f)). However, minimal deposition of extracellular matrix was observed in medial layer of sham-operated mice (Figure 3(e)). Moreover, the aortic wall was structurally similar to unoperated mice (Figure 3(d)). The expression of SM alpha-actin in sham-operated animals was moderately downregulated in the medial elastin layer (Figure 3(h)). By contrast, SM alpha-actin was significantly downregulated in the elastase-perfused animals, especially in the original medial elastin layer (Figure 3(i)). However, a newly generated SMC alpha-actin positive layer without elastin sheets (i.e., neointima) was observed on the luminal side of the damaged media.

3.2. Aortic Luminal Diameter Measurement. All luminal measurements by each method are shown in Table 1. The mean ALD and the range in unoperated mice were 0.57 ± 0.01 mm, 0.11 mm by VM; 0.61 ± 0.01 mm, 0.13 mm by US; 0.43 ± 0.01 mm, 0.13 mm by histology. The mean ALD

Table 1: Summary of the results.

	Control Group			Elastase Group		
Sub Group	VM	US	Histology	VM	US	Histology
Unoperated	0.520	0.586	0.382	0.886	0.880	0.779
Unoperated	0.541	0.623	0.409	1.010	1.075	0.807
Unoperated	0.542	0.552	0.362	1.019	0.997	0.925
Unoperated	0.552	0.606	0.427	1.048	0.921	0.785
Unoperated	0.553	0.626	0.425	1.081	1.093	0.876
Unoperated	0.579	0.586	0.436	1.190	1.154	1.167
Unoperated	0.581	0.623	0.407	1.201	1.074	0.890
Unoperated	0.593	0.606	0.447	1.202	1.348	1.248
Unoperated	0.614	0.634	0.478	1.206	1.153	0.987
Unoperated	0.634	0.684	0.489	1.225	1.331	1.081
Sham	0.653	0.684	0.561	1.265	1.132	0.955
Sham	0.682	0.743	0.576	1.268	1.210	1.077
Sham	0.712	0.735	0.632	1.277	1.273	1.220
Sham	0.721	0.712	0.603	1.330	1.412	1.200
Sham	0.723	0.765	0.599	1.349	1.367	1.131
Sham	0.731	0.756	0.565	1.357	1.486	1.375
Sham	0.764	0.820	0.579	1.381	1.427	1.150
Sham	0.775	0.781	0.534	1.407	1.355	1.200
Sham	0.782	0.812	0.610	1.452	1.562	1.340
Sham	0.789	0.879	0.711	1.762	1.761	1.440

and the range in sham-operated mice were 0.73 ± 0.01 mm, 0.14 mm by VM; 0.77 ± 0.02 mm, 0.20 mm by US; 0.60 ± 0.02 mm, 0.18 mm by histology. The mean ALD and the range in mice perfused with elastase were 1.25 ± 0.04 mm, 0.88 mm by VM; 1.25 ± 0.05 mm, 0.88 mm by US; 1.08 ± 0.05 mm, 0.66 mm by histology. Given that the unoperated and sham-operated aortas have similar structural characteristics, and that the range of values measured by VM, US, and histology were in close proximity, these two groups were combined for subsequent analyses and denoted as the Control group.

3.3. Correlation (Linear Association) and Agreement. The ALD measurements by each measurement in the Control and Elastase groups were normally distributed, respectively. The ALD measurements by US show excellent linear association with VM in both Control and Elastase groups (r = 0.96 and 0.93, 95% CI, resp.). In addition, the US-derived ALD measurements show excellent linear association with histological ALD measures in both Control and Elastase groups (r = 0.92 and 0.93, 95% CI, resp.).

The ICC for ALD measurements obtained for the Control (0.88; 95% CI = 0.72–0.95) and the Elastase (0.92; 95% CI = 0.82–0.97) groups confirmed a high level of agreement between US and VM measurements of assessing aortic diameter across a broad range. By comparison, US and histology measurements of ALD demonstrated a lower level of agreement (Control group ICC = 0.02; 95% CI = −0.41–0.43; Elastase group ICC = 0.66; 95% CI = 0.33–0.85).

Bland-Altman analyses of US and VM measurements in Control (Figure 4(a)) and Elastase (Figure 4(b)) groups indicate that points are all within the limit of agreement, indicating high correlation between the two methods. The average US measurement in control group was significantly above the zero line indicating a trend to overestimate ALD with respect to VM. Bland-Altman analyses of US compared with histological measurements in the Control and Elastase groups are shown in Figure 4(c) and 4(d), respectively. Most points in both groups are in the limit of agreement, indicating good agreement with histological measurements. Once again, average US measurements in both groups were significantly above the zero line indicating a trend to overestimate ALD with respect to histological assessment.

3.4. Comparison of Means. Paired sample t-test confirms the trends observed in the Bland-Altman analysis (Table 2). US measurements in Elastase group shows a nonsignificant trend to overestimate ALD compared with VM measurement, whereas US measurements in Control group significantly overestimated ALD compared to VM (mean bias = 0.039 mm, 95% CI = 0.026–0.051 mm, $P < .001$). This tendency of US to overestimate ALD in the Control group was evident even when unoperated and sham-operated control mice were analyzed separately. (Unoperated mean bias = 0.042 mm, 95% CI = 0.022–0.062 mm, $P < .001$; Sham-operated mean bias = 0.035mm, 95% CI = 0.015–0.056 mm, $P < .05$.) US also overestimated ALD in both groups compared to histological measurements. (Control group mean bias = 0.179 mm, 95% CI = 0.161 to 0.197 mm,

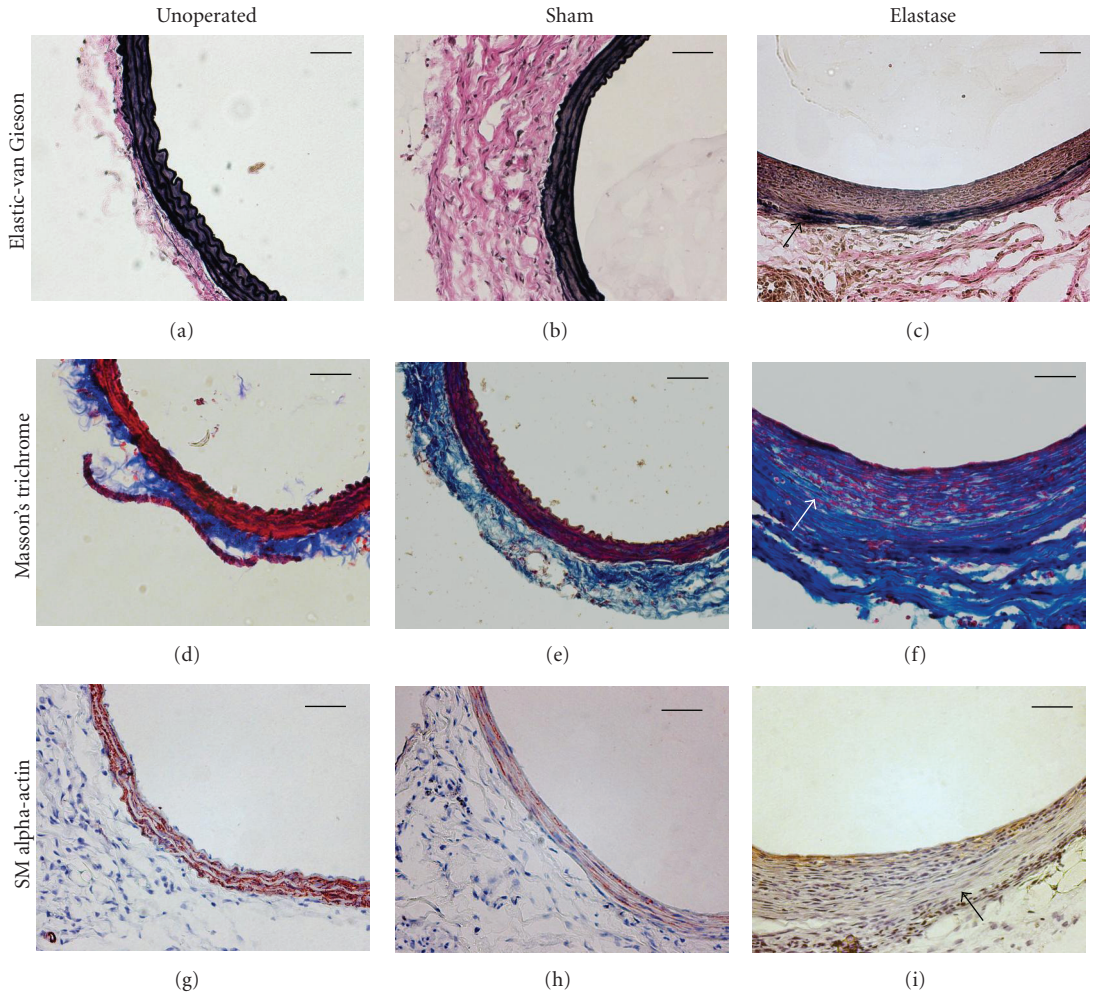

Figure 3: Immunohistochemical evaluation of aorta in unoperated as well as saline or elastase (28 day) perfused mice. Elastic van Gieson staining ((a), (b), (c)) demonstrated destruction of the medial elastin layer in elastase animals ((c), arrow). Masson's trichrome stain ((d), (e), (f)) shows enhanced deposition of extracellular matrix among SMCs in elastase-treated animals ((f), arrow). SM alpha-actin content, as denoted by red staining, is significantly reduced in injured vessels of original medial layer ((i), arrow) compared to Unoperated (g) and Sham controls (h). Black bars = 50 μm

$P < .001$; Elastase group mean bias = 0.170 mm, 95% CI = 0.130–0.208 mm, $P < .001$.)

3.5. Linear Regression. Linear regression analysis of US (x) with respect to VM (y) measurements (Figures 5(a) and 5(b)) reveals excellent correlation between methods in both groups (R^2 of 0.91 in Control group; 0.86 in Elastase group). Similarly, linear regression analysis of US (x) with respect to histological (y) measurements revealed excellent correlation between methods in both Control ($R^2 = 0.84$; Figure 4(c)) and Elastase ($R^2 = 0.84$; Figure 4(d)) groups.

3.6. Intraobserver Variability. The differences between the two serial US or VM measurements of ALD for each aorta in the Control group were normally distributed. The ICC for the two measurements with US and VM were 0.99 and 0.99, respectively, confirming a high level of agreement. No significant difference was detected by Fisher's Z transformation between the ICCs.

The differences between the two serial US and VM measurements of ALD for each aorta in the Elastase group were also normally distributed. The ICC for the two measurements with US and VM were 0.99 and 0.96, respectively, also confirming a high level of agreement. Fisher's Z transformation showed a slight but significant improvement in ICC for US measurements in the Elastase group compared to VM ($P < .05$).

4. Discussion

Improved imaging technology including high-frequency ultrasound and magnetic resonance imaging has allowed adaptation to small animal models of cardiovascular disease.

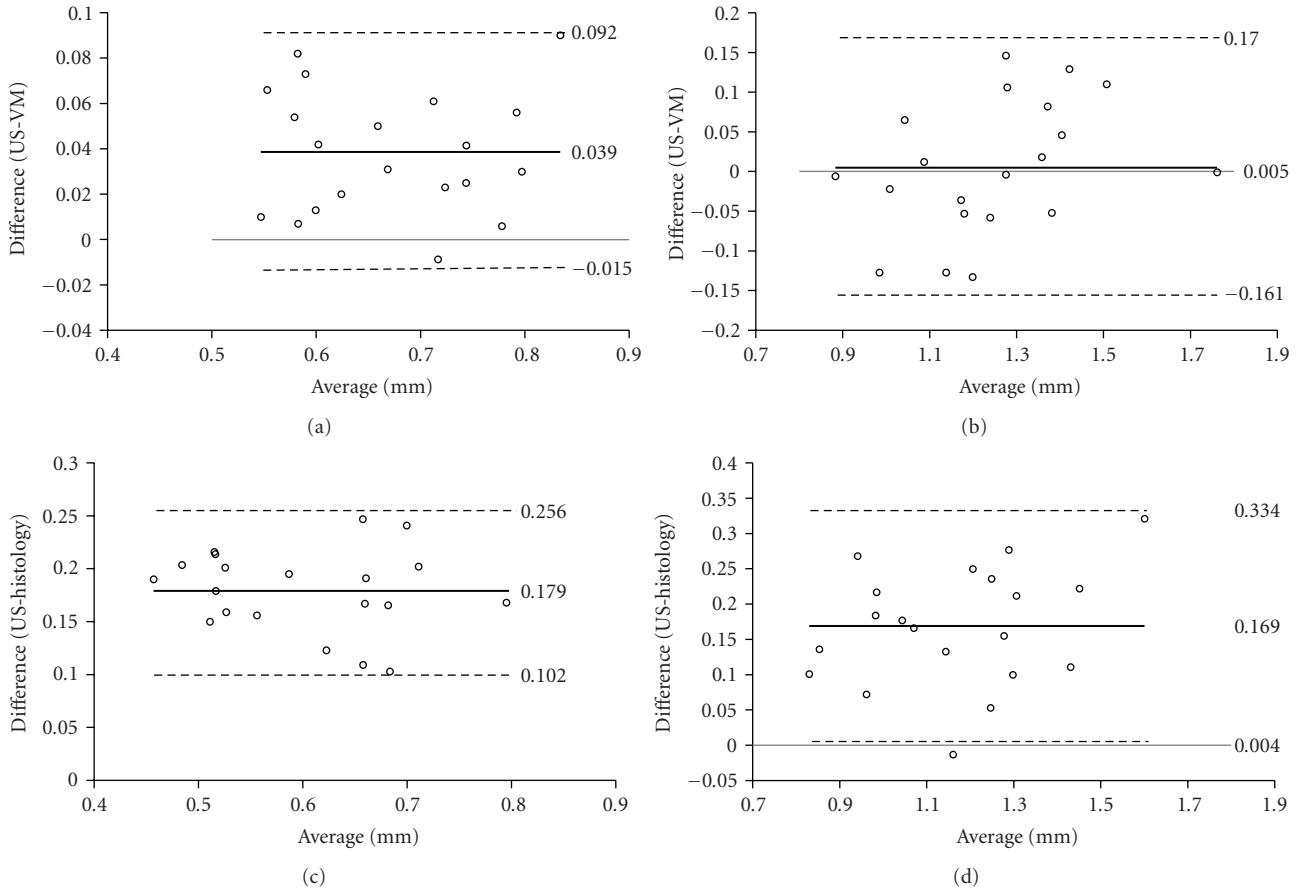

Figure 4: Bland-Altman analyses comparing the US to VM or histological measurements of aortic diameter in Control ((a), (c)) and Elastase ((b), (d)) groups.

Table 2: Paired samples *t*-test for comparison of means.

Paired samples *t*-test	Paired differences			Significance
	Mean	95% CI of the difference		
		Lower	Upper	
ALD by US-ALD by VM in control group	0.039	0.026	0.051	<0.001
ALD by US-ALD by VM in elastase group	0.005	−0.035	0.044	8
ALD by US-ALD by Histology in control group	179	0.161	0.197	<0.001
ALD by US-ALD by Histology in elastase group	0.170	0.13	0.208	<0.001

In addition to ease of measurement, noninvasive imaging modalities allow serial measurements over the time course of disease as well as assessment of therapeutic efficacy. Despite these benefits, direct visualization and *in situ* measurements are still often used to monitor aortic dimensions in models of AAA disease [7, 17]. In the current study, we describe the validity of *in vivo* high-frequency US measurements of ALD in comparison to *in situ* VM in normal murine aorta and elastase-induced AAA.

The current study adds to previous reports that have examined the reliability of ultrasound to monitor AAA development. For example, Martin-Mcnulty et al. [10] demonstrated a high correlation between high-frequency ultrasound and direct postmortem measurements by digital photography of the abdominal aorta while Barisione and colleagues [11] showed similar correlations with morphometric measurements of histology sections. However, both of these studies used the AngII-apoE(−/−) model of AAA development where there are distinctive differences in aneurysm pathology compared to elastase-induced lesions. While grossly similar to human aneurysm, the AngII-apoE(−/−) hyperlipidemic model is now recognized to create focal segmental disruption of elastin resulting in dissections of the suprarenal aorta. The "false" lumens produced by the extending dissections create challenges for accurate assessment of aortic diameter and interpretation of

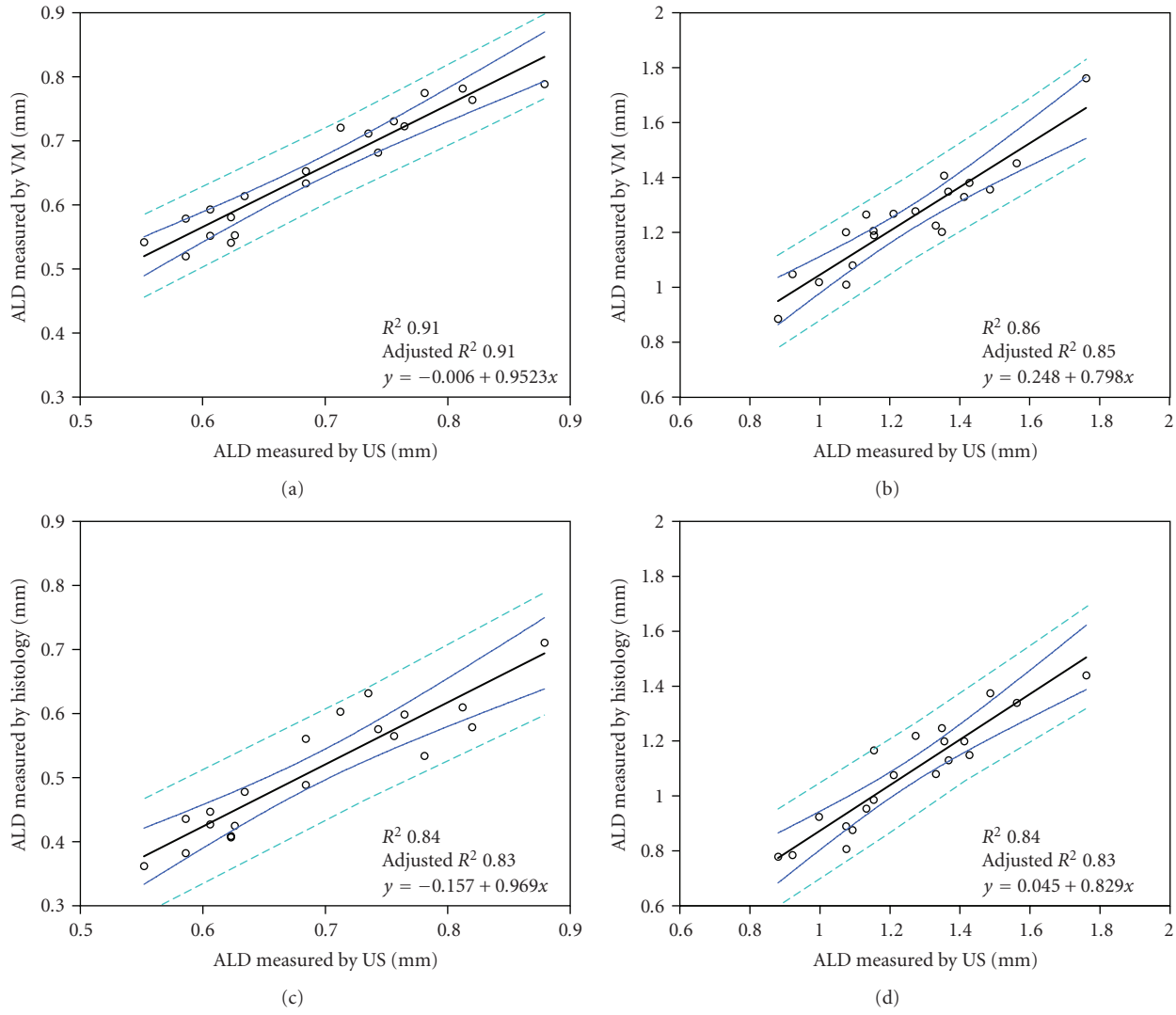

Figure 5: Linear regression of the US measurements (x) with respect to VM or histological measurements (y) in Control (a, c) and Elastase groups (b, d). Lines represent regression line (black), 95% CI for the mean (blue), and 95% CI for the individual measurements (green).

disease etiology. Despite its artificial induction, the elastase-induced AAA model produces a circumferential aneurysm with transmural elastolysis reminiscent of human pathology. Our current data validates the use of high-frequency ultrasound to monitor changes in the inner luminal diameter of the murine abdominal aorta in comparison to *in situ* VM and histological assessment. This is particularly important given that the clinical definition of AAA development is dependent upon luminal diameter expansion. Suffice it to say, it can be generally agreed that no model to date recreates all features of human AAA, but both the AngII-apoE(−/−) and elastase-induced models recreate important characteristics and thus each add valuable insight to disease etiology.

ALD measures using high-frequently US proved to be highly reproducible and were closely correlated with *in situ* VM. While the current data demonstrate that US and VM provide similar information, US yielded statistically significant larger ALD measures in the Control group as compared to VM. Recent noninvasive measurements of ALD using US or MRI in unoperated aorta have also reported larger diameters than those monitored by VM [10, 14, 18, 19]. A potential contributor to the variability in the literature may be the use of nonvolatile anesthetics for VM in previous reports compared to isoflurane used in the current study. Nonvolatile anesthetics such as pentobarbital can impact hemodynamics and reduce blood pressure and cardiac index, whereas isoflurane has fewer such effects [20]. Another potential explanation may be modulation of vascular tone by the surgical procedure to expose the aorta. Prior reports indicate that intraoperative cardiovascular hormones that affect vascular tone, including angiotensin-II, vasopressin and epinephrine, are increased in major abdominal surgery with isoflurane [21]. This could result in enhanced vasoconstriction and decreased aortic diameter.

In contrast to measurements in Control vessels, no significant bias was detected between the methods in the Elastase

group. This may be due to a loss of vascular tone in elastase perfused aorta due fragmentation of elastin sheets and compensatory collagen accumulation during AAA development. Simultaneously, most of the VSMCs in Elastase group lose their contractile phenotype, especially in original medial layer, reducing the ability of the aorta to respond to external vasoactive stimuli [22].

While the current data demonstrate strong correlations between US and histological measures, US yielded statistically significant larger ALD measures in both groups. Also the ICC between US and histology was less than that between US and VM. This phenomenon has been previously attributed to distortion by fixation and staining procedures. Indeed, a so-called "shrinkage index" ($\times 1.25$ for length and $\times 1.56$ for area) has been developed to rectify the procedure-induced changes in dimension [9]. While this index performed well in our Control group ALD measurements, it tended to overcorrect in the Elastase group.

A significant advantage of using noninvasive US imaging is the ability to monitor aneurysm growth over time. This is particularly important given the variability in each of the murine models of AAA described in the literature. The focal breaks in elastin integrity associated with the AngII-apoE(−/−) lead to a large diversity in AAA size as well as histopathology [4]. Diversity in the extent of AAA development has also been described with the elastase-induced model, although these differences are likely due to experimental variables such as the concentration of elastase used as well as the lot-to-lot variations in commercial elastase preparations [17, 23]. In both models, serial monitoring by US can aid in both the optimization of the procedures used as well as proper interpretation of results.

The reproducibility with US was higher than that with VM in experimental AAA. A potential explanation may be the difficulty detecting the luminal edge of the abdominal aorta by VM, in particular with the injured vessel where there is a significant accumulation of connective tissue. From a technical standpoint, optimal visualization of the aortic dimensions by VM requires precise dissection of connective tissue from the aortic wall: insufficient separation can cause underestimation of the inner ALD or overestimation of outer diameter while aggressive cleaning can result in puncture and bleeding which subsequently leads to underestimation of diameter due to decreased blood pressure. In addition to the variability attributed to sample preparation, subsequently harvested aortic samples may not be suitable for further histological analysis, especially of the adventitial region.

Both US and VM measurements have several inherent limitations. Although VM can provide transverse measurements of outer vessel diameter, the anterior midline incision approach does not allow anterioposterior measurements. Similarly, evaluation of inner wall mural thrombus or massive wall thickening by VM is not possible. Since ultrasound measurements using the inner diameter are aided by the discrete blood-wall interface in anterioposterior direction, the elastase model of experimental AAA is particularly suited for this approach as there is not thrombus formation as is often the case with the angiotensin II infusion model [4]. On the other hand, determination of transverse diameters by US is not practical because the blood-wall interface is nearly perpendicular to the transducer surface causing unclear description of the wall (Figures 2(b), 2(d), and 2(e)). This in part explains why it is difficult to measure the outer diameter of the aorta by US as the outer wall does not form as clear an interface with surrounding adventitia despite previous reports [10]. Indeed, the ICC for the outer diameter measurements by US and VM demonstrated reduced correlation compared to that for inner diameter, especially in elastase perfused mice (data not shown).

In summary, we have validated the application high-frequency US imaging to noninvasively measure AAA development in the murine model of elastase-induced AAA. The US system has the advantages of rapid imaging, reproducibility, and high resolution, making possible continuous monitoring of the progression of AAA development over time.

References

[1] A. R. Brady, S. G. Thompson, F. G. R. Fowkes, R. M. Greenhalgh, and J. T. Powell, "Abdominal aortic aneurysm expansion: risk factors and time intervals for surveillance," *Circulation*, vol. 110, no. 1, pp. 16–21, 2004.

[2] R. Pyo, J. K. Lee, J. M. Shipley et al., "Targeted gene disruption of matrix metalloproteinase-9 (gelatinase B) suppresses development of experimental abdominal aortic aneurysms," *Journal of Clinical Investigation*, vol. 105, no. 11, pp. 1641–1649, 2000.

[3] A. C. Chiou, B. Chiu, and W. H. Pearce, "Murine aortic aneurysm produced by periarterial application of calcium chloride," *Journal of Surgical Research*, vol. 99, no. 2, pp. 371–376, 2001.

[4] A. Daugherty, M. W. Manning, and L. A. Cassis, "Angiotensin II promotes atherosclerotic lesions and aneurysms in apolipoprotein E-deficient mice," *Journal of Clinical Investigation*, vol. 105, no. 11, pp. 1605–1612, 2000.

[5] S. Anidjar, J. L. Salzmann, D. Gentric, P. Lagneau, J. P. Camilleri, and J. B. Michel, "Elastase-induced experimental aneurysms in rats," *Circulation*, vol. 82, no. 3, pp. 973–981, 1990.

[6] G. Ailawadi, C. W. Moehle, H. Pei et al., "Smooth muscle phenotypic modulation is an early event in aortic aneurysms," *Journal of Thoracic and Cardiovascular Surgery*, vol. 138, no. 6, pp. 1392–1399, 2009.

[7] M. P. Bergoeing, B. Arif, A. E. Hackmann, T. L. Ennis, R. W. Thompson, and J. A. Curci, "Cigarette smoking increases aortic dilatation without affecting matrix metalloproteinase-9 and -12 expression in a modified mouse model of aneurysm formation," *Journal of Vascular Surgery*, vol. 45, no. 6, pp. 1217–1227, 2007.

[8] E. F. Steinmetz, C. Buckley, M. L. Shames et al., "Treatment with simvastatin suppresses the development of experimental abdominal aortic aneurysms in normal and hypercholesterolemic mice," *Annals of Surgery*, vol. 241, no. 1, pp. 92–101, 2005.

[9] E. Sho, M. Sho, H. Nanjo, K. Kawamura, H. Masuda, and R. L. Dalman, "Hemodynamic regulation of CD34 cell localization and differentiation in experimental aneurysms," *Arteriosclerosis, Thrombosis, and Vascular Biology*, vol. 24, no. 10, pp. 1916–1921, 2004.

[10] B. Martin-Mcnulty, J. Vincelette, R. Vergona, M. E. Sullivan, and YI. X. Wang, "Noninvasive measurement of abdominal aortic aneurysms in intact mice by a high-frequency ultrasound imaging system," *Ultrasound in Medicine and Biology*, vol. 31, no. 6, pp. 745–749, 2005.

[11] C. Barisione, R. Charnigo, D. A. Howatt, J. J. Moorleghen, D. L. Rateri, and A. Daugherty, "Rapid dilation of the abdominal aorta during infusion of angiotensin II detected by noninvasive high-frequency ultrasonography," *Journal of Vascular Surgery*, vol. 44, no. 2, pp. 372–376, 2006.

[12] K. Saraff, F. Babamusta, L. A. Cassis, and A. Daugherty, "Aortic dissection precedes formation of aneurysms and atherosclerosis in angiotensin II-infused, apolipoprotein E-deficient mice," *Arteriosclerosis, Thrombosis, and Vascular Biology*, vol. 23, no. 9, pp. 1621–1626, 2003.

[13] G. H. Turner, A. R. Olzinski, R. E. Bernard et al., "In vivo serial assessment of aortic aneurysm formation in apolipoprotein E-deficient mice via MRI," *Circulation. Cardiovascular imaging*, vol. 1, no. 3, pp. 220–226, 2008.

[14] C. J. Goergen, J. Azuma, K. N. Barr et al., "Influences of aortic motion and curvature onvessel expansion in murine experimental aneurysms," *Arteriosclerosis, Thrombosis, and Vascular Biology*. In press.

[15] J. Azuma, T. Asagami, R. Dalman, and P. S. Tsao, "Creation of murine experimental abdominal aortic aneurysms with elastase," *Journal of Visualized Experiments*, no. 29, 2009.

[16] S. D. Sur, K. Jayaprakasan, N. W. Jones et al., "A novel technique for the semi-automated measurement of embryo volume: an intraobserver reliability study," *Ultrasound in Medicine and Biology*, vol. 36, no. 5, pp. 719–725, 2010.

[17] J. Sun, G. K. Sukhova, M. Yang et al., "Mast cells modulate the pathogenesis of elastase-induced abdominal aortic aneurysms in mice," *Journal of Clinical Investigation*, vol. 117, no. 11, pp. 3359–3368, 2007.

[18] B. S. Knipp, G. Ailawadi, V. V. Sullivan et al., "Ultrasound measurement of aortic diameters in rodent models of aneurysm disease," *Journal of Surgical Research*, vol. 112, no. 1, pp. 97–101, 2003.

[19] S. Amirbekian, R. C. Long, M. A. Consolini et al., "In vivo assessment of blood flow patterns in abdominal aorta of mice with MRI: implications for AAA localization," *American Journal of Physiology*, vol. 297, no. 4, pp. H1290–H1295, 2009.

[20] B. J. A. Janssen, T. De Celle, J. J. M. Debets, A. E. Brouns, M. F. Callahan, and T. L. Smith, "Effects of anesthetics on systemic hemodynamics in mice," *American Journal of Physiology*, vol. 287, no. 4, pp. H1618–H1624, 2004.

[21] A. Goldmann, C. Höehne, G. A. Fritz et al., "Combined vs. Isoflurane/Fentanyl anesthesia for major abdominal surgery: effects on hormones and hemodynamics," *Medical Science Monitor*, vol. 14, no. 9, pp. CR445–CR452, 2008.

[22] T. Boettger, N. Beetz, S. Kostin et al., "Acquisition of the contractile phenotype by murine arterial smooth muscle cells depends on the Mir143/145 gene cluster," *Journal of Clinical Investigation*, vol. 119, no. 9, pp. 2634–2647, 2009.

[23] C. G. Carsten, W. C. Calton, J. M. Johanning et al., "Elastase is not sufficient to induce experimental abdominal aortic aneurysms," *Journal of Vascular Surgery*, vol. 33, no. 6, pp. 1255–1262, 2001.